A Nonlinear Signal Processing Method for Diversity Combining Using Hammerstein Type Filter

Amir Masoud Aminian-Modarres[†, ††] **and Mohammad Molavi-kakhki**[†],
aminian.mod@gmail.com kakhkimol@um.ac.ir
[†] Department of Electrical Engineering, Ferdowsi University of Mashhad, P.O. Box 91775-1111, Mashhad, Iran.
[††] Sadjad Institute of Higher Education, Mashhad, Iran

Summary
Wireless communication systems suffer from the destructive effects of channel fading. In this paper we propose a nonlinear signal processing method for diversity combining based on a Hammerstein type filter to mitigate the fading effects. In the present work, frequency selective Rayleigh fading channels in presence of additive white gaussian noise (AWGN) are considered and BPSK modulation is employed. Comparison of simulation results based on our proposed technique with the results obtained when linear equalizing filters are employed, shows that our technique leads to a considerably better BER performance at higher SNRs. We also show that our method has a lower complexity than the linear structure. Especially, we do not use any memory in our system that is a valuable advantage in many practical applications.

Key words:
Nonlinear signal processing, Hammerstein filter, Wireless communication systems, Diversity combining, Nonlinear equalization

1- Introduction

In wireless communication networks, fading phenomenon imposes serious limitations upon the system performance. Diversity techniques as means of achieving high capacity communication systems and combating fading effects have been the subject of interest for many years [1], [2]. Space, frequency, time and coding diversities, and also the combination of two or more of these, have been investigated by many authors and used in different systems.

At the receiver, the multiple received signals are combined. Various combining techniques have been proposed for flat and frequency selective fading channels [2]-[6]. In presence of additive white gaussian noise, Maximal ratio combining (MRC) is the optimum diversity receiver for flat fading channels, which is a linear technique [2].

In frequency selective channels, the transmitted signal is corrupted by intersymbol interference (ISI) as well as noise. Hence, in these channels, the optimum receiver is based on maximum likelihood sequence estimation (MLSE) method [1]. However, MLSE is a nonlinear method with a high computational complexity that increases exponentially with the channel memory length. As an alternative to MLSE, suboptimum receivers for frequency selective channels have been proposed and used. Linear and decision feedback equalizers (DFE) are the most common techniques [1]. Linear equalizer is simply a linear transversal filter with a limited number of taps, and therefore it is classified as a low complexity technique. Also in DFE, linear transversal filters are employed as feedforward and feedback blocks. Furthermore, in single-input multiple-output (SIMO) frequency selective channels, linear and decision feedback equalizers can be employed in each diversity branch [1].

Other nonlinear equalization techniques have also been proposed. In [7] and [8], techniques using neural networks have been presented. In [9] and [10], another method of equalization based on Volterra series expansion is reported. However the techniques mentioned above suffer from high computational complexity.

In this work we offer a low complexity, memoryless combining technique for SIMO frequency selective Rayleigh fading channels, which is based on Hammerstein type filter. Hammerstein filter is a nonlinear polynomial filter used in many applications such as system identification [11], [12], [13]. Hammerstein decision feedback equalization (HDFE) has been employed in fiber-wireless channel to compensate for nonlinear distortion in the electrical-to-optical converter [14], [15]. HDFE has also been proposed for GSM receivers as an alternative to the existing methods [16]. Moreover blind HDFE has been proposed in order to enhance the spectral efficiency of the system [17]. In these works, single-input single-output (SISO) model is assumed for their communication systems.

This paper is organized as follows. In section 2 we present the system model. Section 3 introduces our nonlinear Hammerstein diversity combining technique. Our simulation results and discussions are presented in section 4. The complexities of nonlinear and linear techniques are compared in section 5, before concluding the paper in section 6.

2- System Model

The equivalent low-pass discrete time model of the system, is illustrated in Fig. 1. In this work we employ BPSK modulation, and the transmitted sequence $x(n) \in \{+1, -1\}$ is drawn from an i.i.d. source with equi-probable symbols.

The SIMO channel consists of M diversity branches. Each branch is assumed to be a frequency selective Rayleigh fading channel, modeled by a tapped delay line with L taps. Hence the channel tap gains can be presented by an $M \times L$ matrix as:

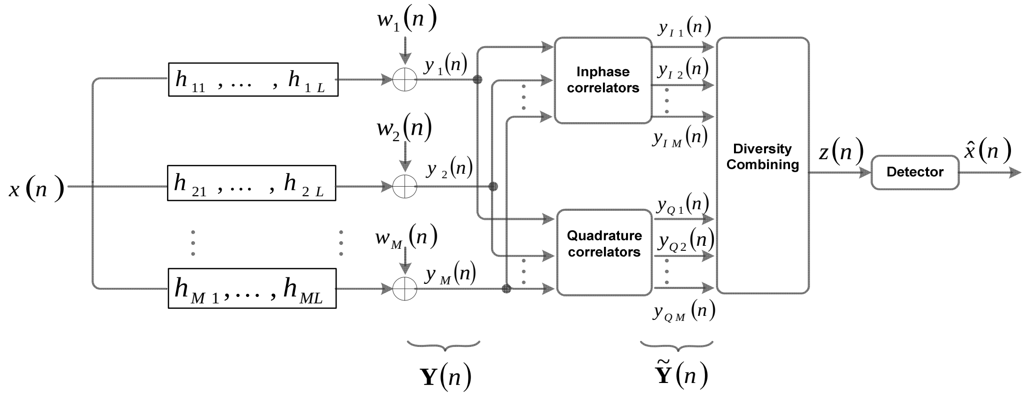

Fig. 1 System model.

$$\mathbf{H} = \begin{bmatrix} h_{11} & h_{12} & \dots & h_{1L} \\ h_{21} & h_{22} & \dots & h_{2L} \\ \vdots & & & \\ h_{M1} & h_{M2} & \dots & h_{ML} \end{bmatrix}, \tag{1}$$

where h_{ij} is the complex Rayleigh distributed random gain of the *j*th tap of the *i*th channel:

$$h_{ij} = h_{Iij} + j\, h_{Qij} \; . \tag{2}$$

h_{Iij} and h_{Qij} are the real and the imaginary component of the channel gain respectively. These two components are independent, zero mean, gaussian random variables with variance σ_h^2. Furthermore, the tap gains are assumed uncorrelated and normalized to unity, i.e. :

$$E\left\{ h_{ij} h_{kl}^{*} \right\} = 0 \quad for \;\; i \neq k \;\, or \;\, j \neq l \; , \tag{3}$$

and:

$$\sum_{j=1}^{L} \left| h_{ij} \right|^2 = 1 \qquad for \quad i = 1, 2, \dots, M \; . \tag{4}$$

In this work the channel fading is assumed sufficiently slow, such that the tap gains do not vary during one data frame. We also assume that the M frequency selective channels have identical power delay profiles (PDP). PDP is the profile of the mean square values of the tap gains. Two examples of exponentially decaying profiles used in our simulations will be shown in Fig 5.

The received signal from the *i*th channel which is corrupted by ISI and noise is given by:

$$y_i(n) = \sum_{j=1}^{L} h_{ij}\, x(n - j + 1) + w_i(n) \qquad for \;\; i = 1, 2, \dots, M, \tag{5}$$

where $w_i(n)$ is the additive white complex gaussian noise at the *i*th receiver branch:

$$w_i(n) = w_{Ii}(n) + j\, w_{Qi}(n) \; . \tag{6}$$

$w_{Ii}(n)$ and $w_{Qi}(n)$ are uncorrelated, zero mean, gaussian random variables with variance σ_w^2. Equation (5) can be expressed in matrix form:

$$\mathbf{Y}(n) = \mathbf{H}\,\mathbf{X}(n) + \mathbf{W}(n), \tag{7}$$

where $\mathbf{H}$ is the channel matrix and $\mathbf{Y}(n)$, $\mathbf{X}(n)$ and $\mathbf{W}(n)$ are the received data vector, the transmitted data vector and the noise vector respectively. These vectors are defined as follows:

$$\mathbf{Y}(n) = [\,y_1(n) \dots y_M(n)\,]^{\mathbf{T}}, \tag{8}$$

$$\mathbf{X}(n) = [\,x(n) \quad x(n-1) \dots x(n - L + 1)\,]^{\mathbf{T}}, \tag{9}$$

$$\mathbf{W}(n) = [\,w_1(n) \dots w_M(n)\,]^{\mathbf{T}}. \tag{10}$$

As shown in Fig. 1, the receiver consists of two correlators banks, namely, inphase and quadrature correlators. The complex received signal $y_i(n)$ from each branch is applied to both correlators. The outputs of the inphase and quadrature correlators are the real part $\left(y_{Ii}(n) \right)$ and the imaginary part $\left(y_{Qi}(n) \right)$ of $y_i(n)$ respectively. According to equations (2) and (6), we can write:

$$y_{Ii}(n)=\sum_{j=1}^{L} h_{Iij}\, x(n-j+1)+w_{Ii}(n),$$
$$y_{Qi}(n)=\sum_{j=1}^{L} h_{Qij}\, x(n-j+1)+w_{Qi}(n), \quad for \quad i=1,2,\dots,M. \tag{11}$$

We define the $2M\times1$ real vector $\tilde{\mathbf{Y}}(n)$ as:

$$\tilde{\mathbf{Y}}(n)=\left[\tilde{y}_1(n)\ \ \tilde{y}_2(n)\ \ \dots\ \ \tilde{y}_{2M}(n)\right]^{\mathbf{T}}$$
$$=\left[y_{I1}(n)\ \ \dots\ \ y_{IM}(n)\ \ y_{Q1}(n)\dots\ \ y_{QM}(n)\right]^{\mathbf{T}}, \tag{12}$$

where:

$$\tilde{y}_i(n)=\begin{cases} y_{Ii}(n) & 1\le i\le M \\ y_{Q(i-M)}(n) & M+1\le i\le 2M \end{cases}. \tag{13}$$

This model is very convenient for computational purposes, as we deal with real values only. It is in fact similar to having $2M$ real diversity branches. As shown in Fig. 1, $\tilde{\mathbf{Y}}(n)$ is the input to the diversity combining filters. Then, the output of the combiner, $z(n)$, is applied to a hard detector for making the output decision $\hat{x}(n)$. In section 3 we will propose our new approach for nonlinear Hammerstein technique. However, since we need to compare our results with the linear structure, a brief review of linear technique is presented here.

Linear Diversity Combining Technique (LDC) is shown in Fig. 2. In this technique, a linear transversal filter with L_{eq} taps is employed for each diversity branch. These filters are designed based on the minimum mean square error (MSE) criterion. The output $z_i(n)$ of the *i*th filter is:

$$z_i(n)=\sum_{k=-(L_{eq}-1)/2}^{(L_{eq}-1)/2} g_{ik}\,\tilde{y}_i(n-k), \quad for \quad i=1,2,\dots,2M, \tag{14}$$

where g_{ik} is the *k*th coefficient of the *i*th filter. The output of the linear combiner can then be written as:

$$z(n)=\sum_{i=1}^{2M}\sum_{k=-(L_{eq}-1)/2}^{(L_{eq}-1)/2} g_{ik}\,\tilde{y}_i(n-k)\ . \tag{15}$$

Equation (15) can be expressed in matrix form:

$$z(n)=\mathbf{G}_{\mathbf{L}}^{\mathbf{T}}\,\mathbf{Y}_{\mathbf{L}}(n), \tag{16}$$

where $\mathbf{G}_{\mathbf{L}}$ is a $2ML_{eq}\times1$ vector that consists of coefficients g_{ik}, and $\mathbf{Y}_{\mathbf{L}}(n)$ is a $2ML_{eq}\times1$ vector that define as follows:

$$\mathbf{Y}_{\mathbf{L}}(n)=\left[\tilde{\mathbf{Y}}^{\mathbf{T}}\left(n+\frac{L_{eq}-1}{2}\right)\ \dots\ \tilde{\mathbf{Y}}^{\mathbf{T}}(n)\ \dots\ \tilde{\mathbf{Y}}^{\mathbf{T}}\left(n-\frac{L_{eq}-1}{2}\right)\right]^{\mathbf{T}}, \tag{17}$$

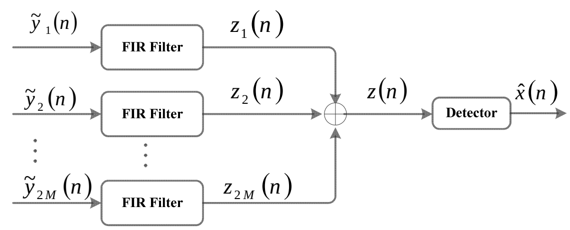

Fig. 2 Linear Diversity Combining Technique (LDC).

where $\tilde{\mathbf{Y}}(n)$ is defined in equation (12). We can obtain the coefficients of LDC by using the MSE criterion:

$$\mathbf{G}_{\mathbf{L}_{opt}}=\mathbf{R}_{\mathbf{L}}^{-1}\,\mathbf{P}_{\mathbf{L}}, \tag{18}$$

where $\mathbf{P}_{\mathbf{L}}$ is the crosscorrelation vector:

$$\mathbf{P}_{\mathbf{L}}=E\left\{\mathbf{Y}_{\mathbf{L}}(n)\,x(n)\right\}, \tag{19}$$

and $\mathbf{R}_{\mathbf{L}}$ is the autocorrelation matrix:

$$\mathbf{R}_{\mathbf{L}}=E\left\{\mathbf{Y}_{\mathbf{L}}(n)\,\mathbf{Y}_{\mathbf{L}}^{\mathbf{T}}(n)\right\}. \tag{20}$$

3- Nonlinear Hammerstein Combining Technique

3-1 Combiner Model

In this section we introduce our memoryless nonlinear Hammerstein Diversity Combining technique (HDC), which is based on utilization of nonlinear Hammerstein type filters. Nonlinearity of the optimum receiver in frequency selective channels, is the motivation of this idea. As show in Fig. 3, in this approach a Hammerstein filter of order D, is employed for each diversity branch. The output polynomial of the *i*th filter is:

$$z_i(n)=\sum_{k=1(k\ odd)}^{D}\hat{g}_{ik}\,\tilde{y}_i^{\,k}(n), \quad for \quad i=1,2,\dots,2M, \tag{21}$$

where $\hat{g}_{ik}$ is the *k*th coefficient of the output polynomial of the *i*th filter, and $\tilde{y}_i(n)$ is defined by equation (13).

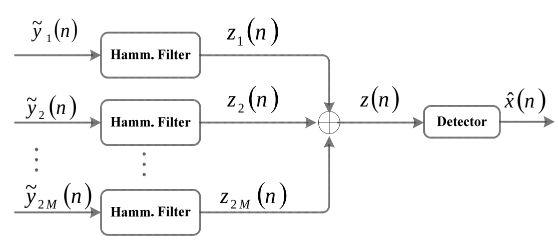

Fig. 3 Hammerstein Diversity Combining Technique (HDC).

Note that since our system is memoryless, no delay term appears in equation (21). Also note that only odd powers exist in the summation of equation (21). We will prove in the next subsequent section that the terms corresponding to the even powers are equal to zero.
The filters outputs are summed to produce the combiner output $z(n)$, i.e. :

$$z(n)=\sum_{i=1}^{2M} \sum_{k=1(k\ odd)}^{D} \hat{g}_{ik}\ \tilde{y}_i^{\,k}(n)\ . \qquad (22)$$

Equation (22) can be expressed in matrix form:

$$z(n)=\mathbf{G_H^T}\ \mathbf{Y_H}(n), \qquad (23)$$

where $\mathbf{G_H}$ is a $M(D+1)\times 1$ vector that consists of coefficients $\hat{g}_{ik}$, and $\mathbf{Y_H}(n)$ is a $M(D+1)\times 1$ vector that define as follows:

$$\mathbf{Y_H}(n)=\left[\tilde{\mathbf{Y}}_\mathbf{1}^\mathbf{T}(n)\ \ \tilde{\mathbf{Y}}_\mathbf{3}^\mathbf{T}(n)\ \ \tilde{\mathbf{Y}}_\mathbf{5}^\mathbf{T}(n)\ \ \ldots\ \ \tilde{\mathbf{Y}}_\mathbf{D}^\mathbf{T}(n)\right]^\mathbf{T},\quad D\ \ odd\,, \qquad (24)$$

where $\tilde{\mathbf{Y}}_\mathbf{p}(n)$ is defined as the *p*th power of $\tilde{\mathbf{Y}}(n)$:

$$\tilde{\mathbf{Y}}_\mathbf{p}(n)=\left[\tilde{y}_1^{\,p}(n)\ \ \tilde{y}_2^{\,p}(n)\ \ \ldots\ \ \tilde{y}_{2M}^{\,p}(n)\right]^\mathbf{T}. \qquad (25)$$

$z(n)$ is an estimate of the transmitted symbol $x(n)$. Our goal is to find the coefficients $\hat{g}_{ik}$ such that the mean square error is minimized.

3-2 Calculation of the Coefficients

The coefficients of the Hammerstein filters are found from the training mode by using the MSE criterion. As shown in Fig. 4, the transmitter sends a training sequence that is assumed to be known to the receiver as the desired signal $d(n)$. The error signal is defined as difference between the desired and estimated values:

$$e(n)=d(n)-z(n)=x(n)-z(n)\,. \qquad (26)$$

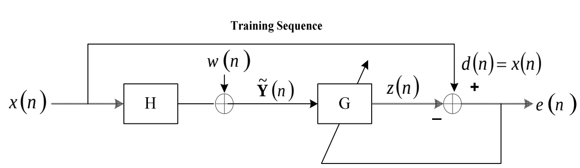

Fig. 4 Training mode.

The cost function is defined as below:

$$\zeta=E\left\{e^2(n)\right\}, \qquad (27)$$

where $E\{.\}$ denotes the statistical expectation. The coefficients are computed such that to minimize ζ .
Using equations (23) and (26) in (27), we get:

$$\zeta=E\left\{\left[\ x(n)-\mathbf{G_H^T}\mathbf{Y_H}(n)\right]\left[\ x(n)-\mathbf{Y_H^T}(n)\mathbf{G_H}\ \right]\right\}. \qquad (28)$$

Expanding the right-hand side of (28), we obtain:

$$\begin{aligned}\zeta &= E\left\{x^2(n)\right\}-\mathbf{G_H^T}E\left\{\mathbf{Y_H}(n)\,x(n)\right\}\\ &-E\left\{x(n)\mathbf{Y_H^T}(n)\right\}\mathbf{G_H}+\mathbf{G_H^T}E\left\{\mathbf{Y_H}(n)\,\mathbf{Y_H^T}(n)\right\}\mathbf{G_H}\end{aligned}\ . \qquad (29)$$

If we define the $M(D+1)\times 1$ crosscorrelation vector:

$$\mathbf{P_H}=\ E\left\{\mathbf{Y_H}(n)\,x(n)\right\}, \qquad (30)$$

and the $M(D+1)\times M(D+1)$ autocorrelation matrix:

$$\mathbf{R_H}=\ E\left\{\mathbf{Y_H}(n)\,\mathbf{Y_H^T}(n)\right\}, \qquad (31)$$

and note that $E\left\{x(n)\mathbf{Y_H^T}(n)\right\}=\mathbf{P_H^T}$, $\mathbf{G_H^T}\mathbf{P_H}=\mathbf{P_H^T}\mathbf{G_H}$, and $E\left\{x^2(n)\right\}=1$, we obtain:

$$\zeta=1-2\,\mathbf{G_H^T}\ \mathbf{P_H}+\mathbf{G_H^T}\ \mathbf{R_H}\ \mathbf{G_H}\,. \qquad (32)$$

This is a quadratic function of vector $\mathbf{G_H}$ with a single global minimum [18]. To minimize ζ , we need to have:

$$\frac{\partial\,\zeta}{\partial\,g_{H\,j}}=0\,, \qquad for\quad j=1,2,\ldots,M(D+1). \qquad (33)$$

These equations may collectively be written as:

$$\nabla\,\zeta=\mathbf{0}\,, \qquad (34)$$

where ∇ is the gradient operator. From equations (32) and (34) and using the gradient properties we can write:

$$\nabla\,\zeta=2\,\mathbf{R_H}\ \mathbf{G_H}-2\,\mathbf{P_H}=\mathbf{0}\ \ . \qquad (35)$$

Finally, the coefficients of Hammerstein filters are obtained by solving (35):

$$\mathbf{G_{H}}_{opt}=\mathbf{R_H^{-1}}\ \mathbf{P_H}\,, \qquad (36)$$

assuming that $\mathbf{R_H}$ is invertible.

3-3 Analysis of the Coefficients

In this section we prove that the even coefficients in equation (22) are equal to zero. To do so, we consider the case where $M=2$, $D=3$, and the channel memory length $L=2$, and assume real channel and noise for simplicity. However, these assumptions do not change the generality and our proof is valid for all cases.
In this case the two received signals are:

$$\begin{aligned} y_1(n) &= h_{11}x(n) + h_{12}x(n-1) + w_1(n), \\ y_2(n) &= h_{21}x(n) + h_{22}x(n-1) + w_2(n). \end{aligned} \quad (37)$$

Also, from our basic assumptions in this work, we have:

$$E\left\{x^k(n)\right\} = \begin{cases} 0 & \text{if } k \text{ is odd} \\ 1 & \text{if } k \text{ is even} \end{cases}, \quad (38)$$

and:

$$E\left\{w_i^k(n)\right\} = \begin{cases} 0 & \text{if } k \text{ is odd} \\ n.z.v. & \text{if } k \text{ is even} \end{cases}, \quad (39)$$

where $n.z.v.$ is a none-zero value. From equations (37)-(39), it is easy to show that:

$$E\left\{y_i^k(n)\, y_j^l(n)\right\} = \begin{cases} 0 & \text{if } (k+l) \text{ is odd} \\ n.z.v. & \text{if } (k+l) \text{ is even} \end{cases}, \quad (40)$$

and:

$$E\left\{y_i^k(n)\, x(n)\right\} = \begin{cases} 0 & \text{if } k \text{ is odd} \\ n.z.v. & \text{if } k \text{ is even} \end{cases}. \quad (41)$$

For real values of channel and noise we have: $\tilde{y}_1(n) = y_1(n)$, and $\tilde{y}_2(n) = y_2(n)$. Hence, equation (24) becomes:

$$\mathbf{Y_H}(n) = \left[y_1(n) \quad y_2(n) \quad y_1^2(n) \quad y_2^2(n) \quad y_1^3(n) \quad y_2^3(n) \right]^{\mathbf{T}}. \quad (42)$$

Substituting equations (40) and (42) in (31), the following form for the autocorrelation matrix is obtained:

$$\mathbf{R_H} = \begin{bmatrix} n.z.v. & n.z.v. & 0 & 0 & n.z.v. & n.z.v. \\ n.z.v. & n.z.v. & 0 & 0 & n.z.v. & n.z.v. \\ 0 & 0 & n.z.v. & n.z.v. & 0 & 0 \\ 0 & 0 & n.z.v. & n.z.v. & 0 & 0 \\ n.z.v. & n.z.v. & 0 & 0 & n.z.v. & n.z.v. \\ n.z.v. & n.z.v. & 0 & 0 & n.z.v. & n.z.v. \end{bmatrix}, \quad (43)$$

where the blocks of the matrix are alternatively zero and none-zero. It is easy to show that the inverse matrix $\mathbf{R_H^{-1}}$ has also a similar form.

On the other hand, substituting equations (41) and (42) in (30), the following form for the crosscorrelation vector is obtained:

$$\mathbf{P_H} = \left[n.z.v. \quad n.z.v. \quad 0 \quad 0 \quad n.z.v. \quad n.z.v. \right]^{\mathbf{T}}. \quad (44)$$

If we substitute $\mathbf{R_H^{-1}}$ and $\mathbf{P_H}$ in equation (36), we have:

$$\mathbf{G_{H}}_{opt} = \left[n.z.v. \quad n.z.v. \quad 0 \quad 0 \quad n.z.v. \quad n.z.v. \right]^{\mathbf{T}}. \quad (45)$$

Hence, the even coefficients of the filter are zero. This proof can be easily generalized for arbitrary values of M, D and L.

3-4 Approximated Coefficients

Equations (18) and (36) imply that some statistical averages must be known for calculating the filters in HDC and LDC techniques. In practice we suppose that our random processes are ergodic, and therefore replace the statistical averages by the corresponding time averages. So, if we assume that the number of the training bits is N_l, $\mathbf{P_H}$, $\mathbf{R_H}$, $\mathbf{P_L}$, and $\mathbf{R_L}$ are estimated as :

$$\hat{\mathbf{P}}_{\mathbf{H}} = \frac{1}{N_l} \sum_{n=1}^{N_l} \mathbf{Y_H}(n)\, x(n), \quad (46)$$

$$\hat{\mathbf{R}}_{\mathbf{H}} = \frac{1}{N_l} \sum_{n=1}^{N_l} \mathbf{Y_H}(n)\, \mathbf{Y_H}^T(n), \quad (47)$$

$$\hat{\mathbf{P}}_{\mathbf{L}} = \frac{1}{N_l} \sum_{n=1}^{N_l} \mathbf{Y_L}(n)\, x(n), \quad (48)$$

$$\hat{\mathbf{R}}_{\mathbf{L}} = \frac{1}{N_l} \sum_{n=1}^{N_l} \mathbf{Y_L}(n)\, \mathbf{Y_L}^T(n) \;. \quad (49)$$

By replacing these estimated values in equations (18) and (36), we obtain an approximation for the coefficients of the filters.

4- Simulation Results and Discussions

In this section the average error rate is evaluated numerically for HDC and LDC techniques and the results are compared. To make use of the advantages of both diversity systems, a hybrid combining technique is also proposed.
The simulations are performed for two different frequency selective Rayleigh channels with exponentially decaying power delay profiles shown in Fig. 5. These are the examples of common profiles used in wireless communication channels [2]. We generate 100,000 random realizations of the channel and obtain the average BER results by Monte Carlo

simulations. We also use a 100-bit sequence for training mode.

4-1- Average BER Performance

In Fig. 6, the average BER versus SNR is shown for HDC and LDC techniques with the channel profile (a). In these simulations, which are performed for three different number of diversity branches $M \in \{2,3,4\}$, we choose the order of Hammerstein filter $D=5$ and the number of linear filter taps $L_{eq}=5$. Fig. 7 shows the results of similar simulations which are performed for the channel profile (b). In these simulations the number of diversity branches are $M \in \{3,4\}$, and we choose $D=5$, and $L_{eq}=7$. From these figures, we observe that at higher SNRs HDC has a considerable better performance than LDC. For example, for $M=4$, when the $SNR = 40\,dB$, the average BER of HDC is 10,000 times lower than LDC, which is a valuable advantage of our proposed technique. However, the disadvantage of HDC at low SNRs, is due to the inherent property of all nonlinear systems at low signal to noise ratios. Examples of these behaviors are observed in decision feedback equalizers, and FM modulators, in which their superiority over linear techniques appears when SNR is above a threshold.

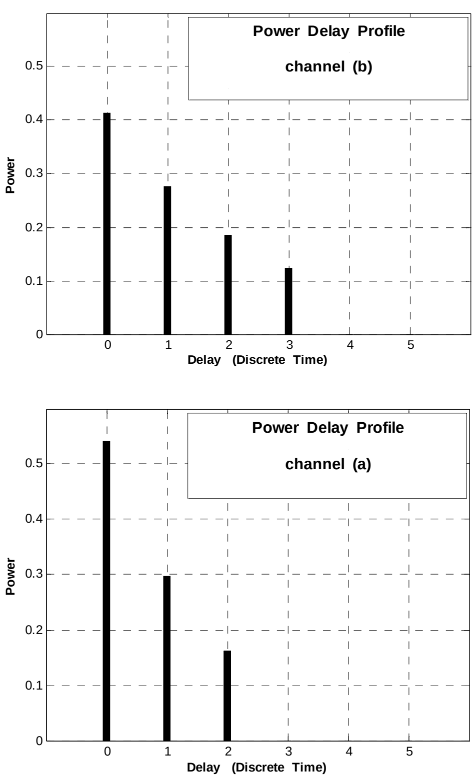

Fig. 5 Two examples for channel PDP.

To prove the validity of the above comparison when the number of taps in LDC is increased, we evaluate the average BER of this technique for different number of taps $L_{eq} \in \{5,7,9,13\}$ and $M=3$ for the channel (b). As can be seen from Fig. 8, the performance dose not change considerably when Leq is increased. Hence, increasing the number of taps in LDC, does not change the superiority of HDC.

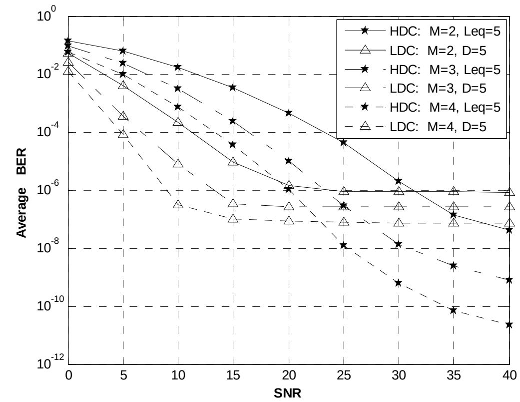

Fig. 6 Average BER performance for the channel (a).

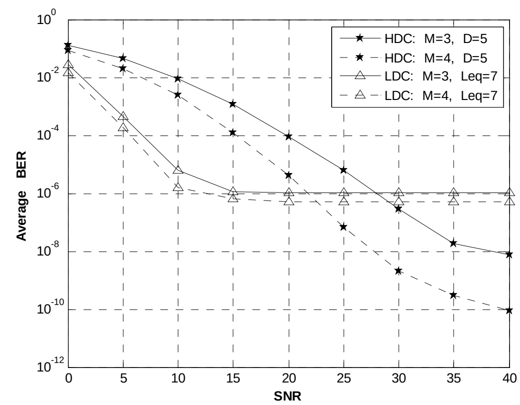

Fig. 7 Average BER performance for the channel (b).

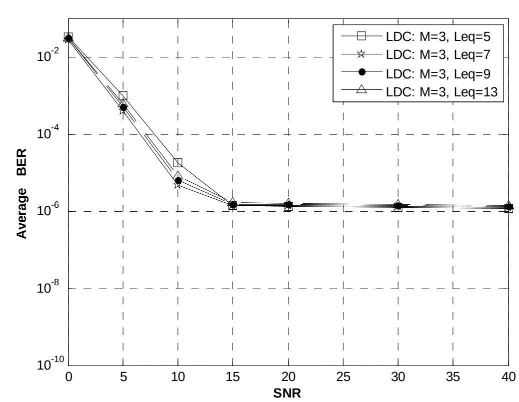

Fig. 8 The effect of increasing the number of taps in LDC (channel b).

To see the effect of the polynomial order D on the performance of HDC, simulations are performed for three different values of $D \in \{3,5,7\}$ and $M = 3$ for the channel (b). The results of these simulations are presented in Fig. 9. As can be seen from this figure, when $D > 5$, the system performance dose not change notably. Hence, in this work we choose $D = 5$.

4-2- Hybrid Technique

Considering the results, we conclude that HDC system has a better performance at higher SNRs, while at lower SNRs the performance of LDC system is better. To make use of the advantages of both systems, we propose a hybrid technique. In this technique as shown in Fig. 10, a simple estimator estimates the value of SNR at the training mode. The receiver is then switched to LDC or HDC mode, according to the estimated SNR. By this method we can obtain a satisfactory performance at all SNRs.

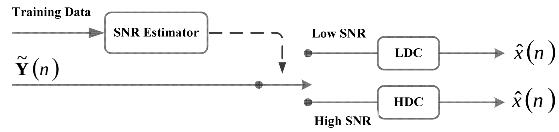

Fig. 10 Hybrid technique.

5- Comparison of HDC and LDC Complexities

LDC technique is known as a low complexity system. In this section we compare the complexity of HDC and LDC techniques and show that HDC has a considerably less complexity.

5-1- Memory Usage

HDC is a memoryless system. This property provides many benefits, like low cost, low power consumption and low hardware complexity. On the other hand, LDC technique requires $2M \times (L_{eq} - 1)$ memories. Especially, for long impulse response channels (high values of L_{eq}) and high values of M, the number of required memories is significant, and therefore the cost and the complexity of the system are increased.

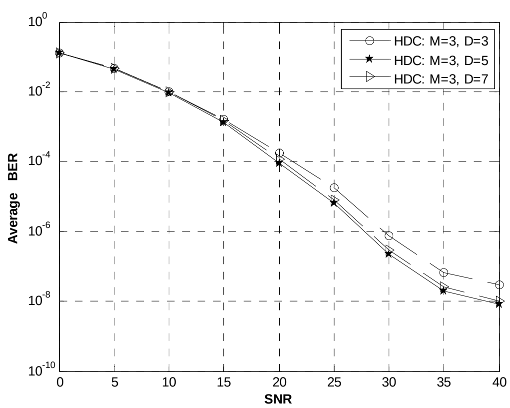

Fig. 9 The effect of increasing polynomial order in HDC (channel b).

5-2- Computational Complexity

The computational complexity of HDC and LDC techniques is proportional to the number of coefficients of their filters. To present a quantitative comparison for computational complexity, we define the *complexity ratio* as:

$$Cxr \overset{\Delta}{=} \frac{The\ number\ of\ taps\ in\ LDC}{The\ number\ of\ taps\ in\ HDC}. \tag{50}$$

From the equations (18) and (36), Cxr becomes:

$$Cxr = \frac{2M\,L_{eq}}{M\,(D+1)}. \tag{51}$$

If we assume that the number of diversity branches is the same for both techniques, we have:

$$Cxr = \frac{2L_{eq}}{(D+1)}. \tag{52}$$

As an example, for $D = 5$ and $L_{eq} = 7, 9, 13$, the complexity ratio is $Crx = 2.33, 3, 4.33$ respectively. This means that the computational complexity of HDC is $2.33, 3, 4.33$ times lower than LDC respectively. This is a significant advantage for HDC technique, especially for long impulse response channels.

5-3- Equipments

Another valuable advantage of HDC technique over LDC is that in this system, we need a lower number of diversity branches. As we can observe from Figs. 6 and 7, at higher SNRs the performance of HDC for a lower number of diversity branches M, is even better than LDC performance with a higher values of M. From Fig. 6 we observe that the performance of HDC for the channel (a) with $M = 3$, is better than the performance of LDC with $M = 4$ when $SNR \geq 27.5\,dB$. Also we observe that in this case the performance of HDC with $M = 2$ is better than the performance of LDC with $M = 4$ when $SNR \geq 38\,dB$.

Hence, we can save the number of diversity branches, by using HDC technique. Consequently the number of antennas (in spatial diversity), correlators and other equipments required in the receiver are decreased.

Table 1: Comparison of HDC with $D=5$ and LDC with $L_q=7$ for the channel (b)

	Average BER	Number of coefficients	Number of Diversity branches	Number of correlators	Memory usage
HDC at SNR = 25 dB	8.8 e -6	18	3	6	0
HDC at SNR = 31 dB	1.6 e -7				
HDC at SNR = 40 dB	8.1 e -9				
LDC at SNR = 25 dB	1.65 e-7	84	6	12	72
LDC at SNR = 31 dB	1.6 e -7				
LDC at SNR = 40 dB	1.5 e -7				

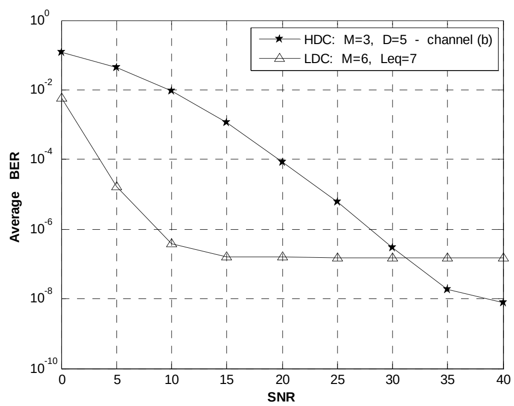

Fig. 11 Average of BER of HDC with $D=5$ and $M=3$ and LDC with $L_q=7$ and $M=6$ for the channel (b)

At the end of this section, we consider a demonstrative example. In Fig. 11, the results of our simulation for HDC with $M=3$ and $D=5$ are compared with LDC with $M=6$ and $L_{eq}=7$ for the channel (b). Conclusions obtained from this comparison are summarized in Table 1.

6- Conclusion

In this paper we introduced a nonlinear low complexity memoryless combining technique based on Hammerstein type filters. We employed BPSK modulation and assumed frequency selective Rayleigh fading channels. The performance of our proposed system was evaluated for different number of diversity branches and polynomial orders. Comparison of our simulation results with the results that we obtained from linear combining technique, shows that:

i) At higher SNRs, the average BER performance of HDC is superior to LDC.
ii) HDC provides a considerable low complexity technique as it needs less number of diversity branches, memories and computations than LDC.
iii) To make use of the advantages of both HDC and LDC systems, a hybrid combining technique was proposed.

References

[1] J. G. Proakis, and M.Salehi, Digital Communications, Fifth ed. New york: McGraw-Hill, 2008.

[2] M. K. Simon, and M. S. Alouini, Digital Communication Over Fading Channels, 2nd ed. New Jersey: John Wiley & Sons, 2005.

[3] H. C. Yang, and M. S. Alouini, "Improving the performance of switched diversity with post-examining selection," IEEE Trans. Wireless Commun., vol. 5, no. 1, pp. 67-71, Jan. 2006.

[4] R. You, H. Li, and Y. Bar-Ness, "Diversity combining with imperfect channel estimation," IEEE Trans. Commun., vol. 53, no. 10, pp. 1655-1662, Oct. 2005.

[5] R. K. Mallik, "Optimized diversity combining with imperfect channel estimation," IEEE Trans. Infor. Theory, vol. 52, no. 3, pp. 1176-1184, Mar. 2006.

[6] A. A. Basri, and T. J. Lim, "Optimum combining in rician / rayleigh fading environment with channel estimation errors," in Proc. IEEE Sym. Communications, Jun. 2006, vol. 1, pp. 274-278.

[7] D. C. Park, and T. K. Jung Jeong, "Complex-bilinear recurrent neural network for equalization of a digital satellite channel," IEEE Trans. Neural Net., vol. 13, no. 3, pp. 711-725, May 2002.

[8] N. Xie, and H. Leung, "Blind equalization using a predictive radial basis function neural network," IEEE Trans. Neural Net., vol. 16, no. 3, pp. 709-720, May 2005.

[9] S. Im, and E. Powers, "Equalization of nonlinear digital satellite channels using a frequency-domain adaptive Volterra filter," in Proc. ISPACS'94, Seoul, Korea, 1994, pp. 7–12.

[10] F. Y. Wang, J. Licheng, and P. Jin, "MIMO Volterra filter equalization using pth-order inverse approach," in Proc. IEEE Conf. ICASSP, 2001, vol. 01, pp. 177-180.

[11] N. Kalouptsidis, and P. Koukoulas, "Blind identification of Volterra-Hammerstein systems," IEEE Trans. on Signal Processing, Vol. 53, Issue 8, Part 1, pp.2777 - 2787, Aug. 2005.

[12] F. Giri, F. Z. Chaoui, M. Haloua, Y. Rochdi, and A. Naitali, "Hammerstein model identification," in Proc. of the 10th Mediterranean Conference on Control and Automation - MED2002, Lisbon, Portugal, July 2002.

[13] G. Picard, O. Capp´e, "Blind identification of Hammerstein nonlinear distortion models," IEEE Workshop on Applications of Signal Processing to Audio and Acoustics, New Paltz, NY Oct. 2003.

[14] X. N. Fernando, A. B. Sesay, “A Hammerstein type equalizer for the Wiener type fiber wireless channel,” in Proc. IEEE Conf. PACRIM '01, Aug. 2001, vol. 1, pp. 546-549.
[15] X. N. Fernando and A. B. Sesay, “A Hammerstein type equalizer for concatenated fiber-wireless uplink,” IEEE Trans. Vehicular Tech., vol. 54, no. 6, pp. 1980–1991, 2005.
[16] Y. Miar, and H. Amindavar, “Hammerstein decision feedback equalization (HDFE) as a new equalizer of GSM receivers,” IEEE International Sym. Signal Processing and its Applications (ISSPA), Paris, France, July 2003.
[17] Y. Miar, A. R. Momen, H. AminDavar and H. Samimi, **“**Blind Hammerstein decision feedback equalizer (BHDFE) as a new blind equalizer,” in proc. IEEE Canadian Conference on Electrical and Computer Engineering, Niagara Falls, Canada, May 2004, Vol. 1, pp. 567- 570.
[18] B. Farhang-Boroujeny, Adaptive Filters, Theory and Applications, Chichester: John Wiley & Sons, 1998.

Amir Masoud Aminian Modarres received the B.S. degree in electronic engineering and the M.S. degree in communication engineering from Ferdowsi University of Mashhad, Iran, in 1995 and 2002, respectively. He is currently working toward the Ph.D. degree at the Ferdowsi University of Mashhad. Since 2002 he has been a faculty member in department of electrical engineering at Sadjad Institute of Higher Education, Mashhad, Iran. His current interests are digital communications, signal processing and cryptography.

Mohammad Molavi Kakhki (S. M. IEEE 1993) received the B.S. degree in physical electronics in 1971 from university of Tabriz, Iran, and M.S. and Ph.D. degrees in electronic communications from University of Kent at Canterbury, UK. in 1977 and 1981 respectively. From 1981 to 1984 he worked as a research fellow at Kent University. In 1985 he joined department of electrical engineering at Ferdowsi University of Mashhad, Iran, and he is currently an associate professor in this university. His current interests are optical communications, digital communications and power line communications.